Machine learning applied to image interiors of Red-giant stars

Siddharth Dhanpal, DAA, TIFR
Advisor: Dr. Shravan Hanasoge, DAA, TIFR

December 2019

1 Introduction

All stars oscillate. These oscillations are standing waves of two kinds, one where pressure is the restoring force (p modes; like sound waves) and other where buoyancy is the restoring force creating (g modes). Studying these waves assists in understanding the structure and rotation of the Sun and other stars, with which we gain insights into processes of stellar evolution. Red giants are unique laboratories, providing a direct view of the complex death of main sequence (solar-like) stars. The seismology of red giant oscillations can be potentially used to infer the interior structure, composition, and the rotation profile. Many aspects like the angular momentum transport and evolution [1], strong magnetic fields [3], and stellar structure change in the red-giant phase[4] contain rich physics are of great interest to astrophysicists.

The *Kepler* mission (2009) has provided an enormous trove of seismic data of thousands of red giants at signal-to-noise ratios ranging from ten to ten thousand [5]. Kepler provides "light curves" for almost 200,000 stars, which are time series of minute fluctuations in their luminosities. Power spectra (squared absolute values of Fourier transforms of these recorded time series) show a sequence of peaks rising above a noisy background. The primary challenge is to label the peaks (using quantum numbers $\{n, \ell, m\}$), enabling the classification of p and g modes, rotation rates of the core and outer envelope and making precision seismology of the interior possible. Simple relationships govern the spacings[6][7] between consecutive peaks of p and g modes but mode identification is complicated by the mixed-mode behaviour that red giants exhibit. Currently Bayesian methods are applied to analyse the spectra - these are difficult to extend to the red-giant spectra[8] and only a machine learning algorithm can potentially overcome these challenges.

2 Stellar Oscillations

Oscillation modes are sensitive to the structure of the host star. These oscillations, treated in the present case as being linear perturbations around the equilibrium state, are resonances, where the resonant frequencies occur only at specific and discrete *eigen frequencies*.

Different regions inside the star have different dominating restoring forces, in turn influencing the eigenfrequencies of the oscillation spectrum. The radial oscillations ξ_r can be described by the equation

$$\frac{\mathrm{d}^2\xi_r}{\mathrm{d}r^2} = -K_s(r)\xi_r, \quad \text{where} \quad K_s(r) = \frac{\omega^2}{c^2}\left(1 - \frac{N^2}{\omega^2}\right)\left(1 - \frac{S_\ell^2}{\omega^2}\right) \tag{1}$$

where c is the sound speed, r is the distance from the centre, ω is the angular frequency of the wave, $S_\ell = \sqrt{\ell(\ell+1)}c/r$ is the lamb frequency and N is is the Brunt-Vaisala frequency given by

$$N^2 = g_0\left(\frac{1}{\Gamma_{1,0}}\frac{\mathrm{d}\ln p_0}{\mathrm{d}r} - \frac{\mathrm{d}\ln \rho_0}{\mathrm{d}r}\right). \tag{2}$$

where g_0 is the magnitude of acceleration due to gravity, p_0 is the equilibrium pressure, ρ_0 is the equilibrium pressure and $\Gamma_{1,0}$ is the first adiabatic exponent at equilibrium ($\Gamma_1 = \frac{\partial \ln p}{\partial \ln \rho}$).

Solutions of ξ_r depend on the sign of $K_s(r)$. If $K_s(r) > 0$, the perturbations are oscillatory and if $K_s(r) < 0$, the perturbations are exponentially decaying and *evanescent*.

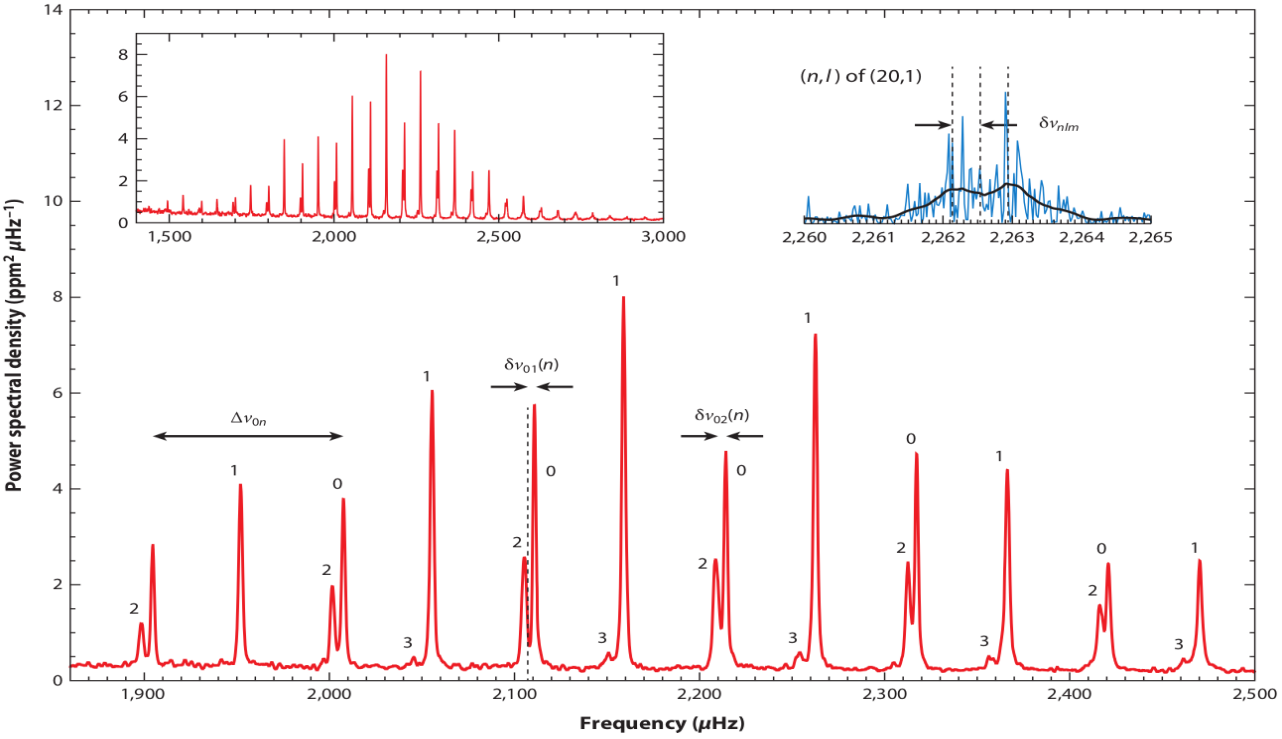

Figure 1: Oscillation spectrum of the G-type main-sequence star in 16 Cyg A (KIC 12069424, HD 186408), as observed by Kepler (figure reproduced from [9]). (*Main plot*) The smoothed frequency spectrum denotes prominent oscillation modes, indicated by degree ℓ on the top of peak. (*Inset, top left*) Wider range plot of frequency showing the gaussian modulation of observed power of modes. (*Inset, top right*) The zoomed-in spectrum shows rotational splitting, where the dashed lines indicate $m = 0$ in the center and $|m|$=1 on either side. The raw spectrum is indicated by blue line and black line indicates smoothed spectrum.

2.1 p modes

p modes are waves for which pressure is the restoring force (acoustic modes). These waves are the most dominant modes of the oscillation in solar-like stars, e.g., the well known 5-minute oscillations of the Sun.

p modes are oscillations occur when the condition $K_s > 0$ is satisfied. These waves are trapped in the region where $|\omega| > |N|$ and $|\omega| > |S_\ell|$. These modes are trapped in the region between inner turning point r_t, where $S_\ell(r_t) = \omega$ and the surface. The WKB analysis [10] for a trapped mode in region (r_1, r_2) gives the following relation,

$$\int_{r_1}^{r_2} K_s(r) = \left(n - \frac{1}{2}\right)\pi, \qquad n = 1, 2, \ldots \tag{3}$$

Extending the analysis for a p mode trapped in (r_t, R) in the asymptotic limit, i.e. $\omega \gg |N|$, we obtain

$$\int_{r_t}^{R} \left(1 - \frac{L^2c^2}{r^2\omega^2}\right)^{\frac{1}{2}} \frac{\mathrm{d}r}{c} = \frac{[n + \alpha(\omega)]\,\pi}{\omega} \tag{4}$$

where $\alpha(\omega)$ accounts for phase change at lower turning point and phase change at the surface.

For low-degree modes, i.e., $\ell \ll n$, r_t is approximately at the centre and the integrand is close to one for most of the range of integration. Considering leading order terms,

$$\nu_{n\ell} = \frac{\omega_{n\ell}}{2\pi} = \left(n + \frac{\ell}{2} + \frac{1}{4} + \alpha\right)\Delta\nu, \tag{5}$$

where

$$\Delta\nu = \left[2\int_0^R \frac{\mathrm{d}r}{c}\right]^{-1}, \tag{6}$$

is the *large frequency separation*, the inverse of twice the sound travel time between the centre and surface. From the expressions of $\nu_{n\ell}$, having the modes with the same value of $n+\ell/2$ have nearly same frequencies and are nearly degenerate, i.e.,

$$\nu_{n\ell} \simeq \nu_{n-1\ell+2} \text{ and } \delta\nu_{n\ell} \equiv \nu_{n\ell} - \nu_{n-1\ell+2} \simeq -(4\ell+6)\frac{\Delta\nu}{4\pi^2\nu_{n\ell}}\int_0^R \frac{\mathrm{d}c}{\mathrm{d}r}\frac{\mathrm{d}r}{r}, \tag{7}$$

where $\delta\nu_{n\ell}$ is called the *small frequency separation*.

We define average quantities of the *large frequency separation* and *small frequency separation* for a better fit of the observed spectrum.

$$\langle\nu_{n+1\ell} - \nu_{n\ell}\rangle_{n\ell} = \Delta\nu_0 \quad \delta\nu_l \equiv \langle\nu_{n\ell} - \nu_{n-1\ell+2}\rangle_n \simeq (4\ell+6)D_0, \tag{8}$$

such that,

$$\nu_{n\ell} \simeq \Delta\nu_0\left(n + \frac{\ell}{2} + \epsilon_0\right) - \ell(\ell+1)D_0, \tag{9}$$

where $\epsilon_0 = \alpha + 1/4$.

Interesting characteristics of p modes are:

- All frequency peaks (resonances) of p modes which have same degree ℓ are approximately spaced uniformly apart by $\Delta\nu_0$.
- The peaks of $\ell = 0$ and $\ell = 2$ modes are in close proximity. Similarly, the peaks of $\ell = 1$ and $\ell = 3$ are closely spaced.
- The parameter *large frequency separation* - $\Delta\nu$ provides a scale of acoustic depth in the star. The parameter small frequency separation - $\delta\nu$ depends on the gradient of sound speed in the core which provides the information of the composition of a star.
- For Sun, these modes are present in the radiative envelope.
- As star evolves into a red giant, $\Delta\nu_0$ decreases [14]. This may be understood because the star expands as it evolves and consequently, the stellar radius increases. Hence, there is a decrease in the *large frequency separation* (Eq. 6) [15] .

2.2 g modes

As the name indicates, g modes are internal gravity waves which are driven by buoyancy, and therefore by gravity. Although they have not been observed directly in the sun, there have been many weak detections of g modes. These waves decay in the convection zone and hence have a very low amplitude at the surface.

g modes are oscillations(i.e., $K_s > 0$) with low frequencies. These waves are trapped in the region where $|\omega| < |N|$ and $|\omega| < |S_\ell|$. For the asymptotic case ($\omega \ll |S_\ell|$), in g modes

$$K_s(r) \simeq \frac{\ell(\ell+1)}{r^2}\left(\frac{N^2}{\omega^2} - 1\right). \tag{10}$$

Extending the WKB analysis in the asymptotic limit of g modes trapped in the region $[r_1, r_2]$, we obtain

$$\int_{r_1}^{r_2}\left(\frac{N^2}{\omega^2} - 1\right)^{1/2}\frac{\mathrm{d}r}{r} = \frac{(n-1/2)\pi}{L}. \tag{11}$$

For high order, low degree ($\ell \ll |n|$) g modes, ω is much less than N for most of the trapped region in $[r_1, r_2]$.

$$\omega = \frac{L\int_{r_1}^{r_2} N\frac{\mathrm{d}r}{r}}{\pi(n+\alpha_{\ell,g})}, \tag{12}$$

where the term $\alpha_{\ell,g}$ accounts for the phase change at boundaries. This equation implies,

$$\Pi = \frac{\Pi_0}{L}(n + \alpha_{\ell,g}) \text{ where } \Pi_0 = 2\pi^2 \left(\int_{r_1}^{r_2} N \frac{\mathrm{d}r}{r} \right)^{-1}. \tag{13}$$

Here, the phase $\alpha_{\ell,g}$ depends on whether core is radiative or convective. For the case of radiative core, $\alpha_{\ell,g} = \ell/2 + \alpha_g$ and for the other case of convective core, $\alpha_{\ell,g} = \alpha_g$ which does not depend on ℓ. In any case, α_g accounts for phase change at turning points. Interesting characteristics of g modes:

- All the periods of g modes with same degree ℓ are asymptotically uniformly spaced apart by $\Delta\Pi_0$
- For the Sun, these modes are present in the radiative core. The parameter Π_0 provides the scale of radiative core size.
- As the star evolves into a red giant, $\Delta\Pi_0$ decreases[14][15].

2.3 Mixed p/g modes

When stars reach the end of main-sequence in the evolution, there is an increase in density gradient, which raises Brunt-Vaisala frequency(N). One of the consequence is that a mode can be trapped in two different regions where it is a p mode in one region and g mode in other region. This mode exhibits the characteristics of both modes for the same eigenfrequency and is hence called mixed mode. Therefore, this mode is oscillatory in two different regions with different characteristics and evanescent in the region that connects these regions. The frequencies of the mixed modes asymptotically are given by solutions of equation:

$$\tan \pi \frac{\nu - \nu_p}{\Delta\nu_p} = q \tan \frac{\pi}{\Delta\Pi_0} \left(\frac{1}{\nu} - \frac{1}{\nu_g} \right) \ , \tag{14}$$

where q is the coupling factor[12].

2.4 Effect of Rotation

Rotation breaks the spherical symmetry of the star and lifts the degeneracy of modes in m. Slow rotation, like as Sun (1.74mhz) may be treated as a perturbation to the non-rotating case [11]. Each mode of degree ℓ is split into $2\ell + 1$ m components. Each mode $\omega_{n,\ell,m}$ is given by $\omega_{n,\ell,m} = \omega_{n,\ell} + \delta\omega_{n,\ell,m}$. Assuming that the star exhibits solid body rotation at rate Ω,

$$\delta\omega_{n,\ell,m} = m\,(C_{n,\ell} - 1)\,\Omega \tag{15}$$

For p modes, $C_{n,\ell} \approx 0$ and for g modes, $C_{n,\ell} \approx 1/\ell(\ell+1)$. Therefore, the multiplets of p modes are given by

$$\nu_{n,\ell,m} = \nu_{n,\ell} - m\nu_s \tag{16}$$

where $\nu_s = \Omega/2\pi$ is called the splitting. If Ω changes with radius, splitting changes as a function of the depth that the mode probes. Due to the presence of mixed modes in the evolved stars like red-giants and sub-giants, the core rotation rate can be inferred as well.

2.5 Detection of Oscillations and Visibility of different modes

Stellar Oscillations can be detected and measured using two fundamental techniques:

1. Doppler Velocity: It is a technique that measures the Doppler velocity of patches on the surface. ESA/NASA *Solar and Heliospheric Observatory* (SoHO) and *Global Oscillations at Low Frequencies* (GOLF) uses this technique.
2. Photometry: It is a technique that measures Intensity/flux of photons using a CCD photometer. *Variability of solar Irradiance and Gravity Oscillations instrument* (VIRGO) and *Kepler* uses this technique.

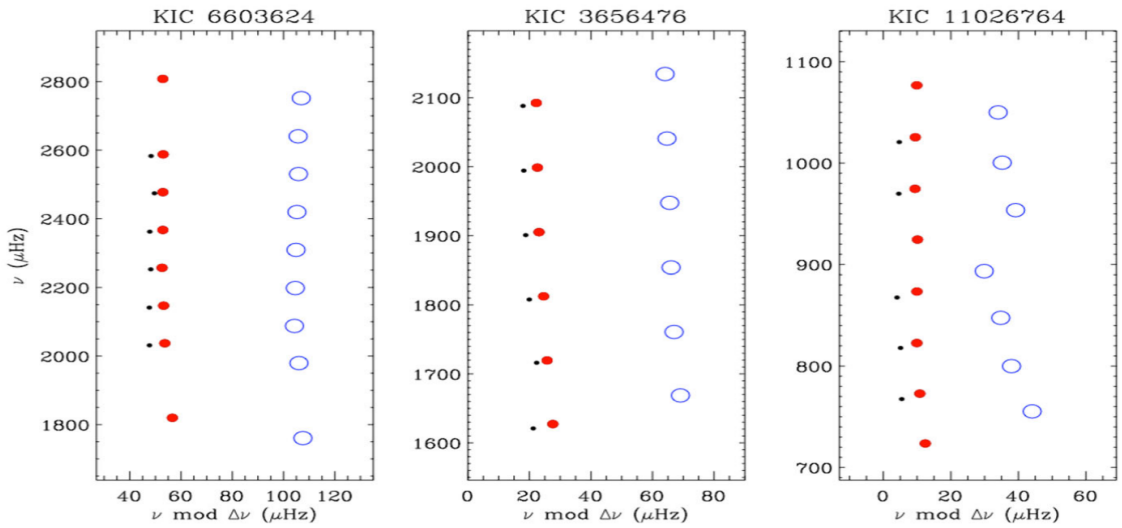

Figure 2: Echelle diagram of 3 stars observed by Kepler [11]. Three ridges here are $\ell = 0$ (filled red symbols), $\ell = 1$ (open blue symbols) and $\ell = 2$ (small black symbols). We don't observe $\ell = 3$ mode due to low visibility and the bump in the right most star indicates a mixed mode.)

The convective background is higher in photometry compared to Doppler-velocity methods [10]. Hence, the SNR is higher in Doppler-velocity measurements ($\sim$ 300) compared to photometric measurements ($\sim$ 30) of oscillations. Using the Doppler velocity technique, it is possible to characterize the stellar oscillations at low frequencies. But photometric techniques work better outside earth's atmosphere (for situations when there is a low photon count). Therefore, the stars that Kepler has characterized is through the application of photometry. **Mode Visibility**: In the case of distant stars with low spatial resolutions, we observe only low degree (ℓ) modes. The visibility of a fluctuation, for a mode $f_{n,\ell,m} = AY_\ell^m(\theta, \phi)$ is given by

$$a_{n,\ell,m} = r_{\ell,m}(\iota) V_\ell A, \tag{17}$$

where V_ℓ is the mode visibility, $r_{\ell,m}(\iota)$ is the relative amplitude of the mode depends on the inclination angle ι. The visibility function depends on the limb-darkening function and the weighting function, which weights the limb darkening function. This weighting function depends on the measurement technique used.

The visibility function V_ℓ is in decreases with increasing degree ℓ. Therefore, we dominantly observe only $\ell = 0, 1$ and 2 modes in the ateroseismic data as the amplitude decreases for other degree modes. We rarely observe $\ell = 3$ modes.

2.6 Spectral Analysis

Traditional methods of analysing the spectra use Echelle diagrams. The Echelle diagram is constructed by cutting the spectrum in parts of size $\Delta\nu_0$ and piling these parts one on top of next. Following the first order asymptotic theory of stellar oscillations, we see the ridges of $\ell = 2, 0, 1, 3$ in an order as in figure 2. But in evolved stars, $\ell = 1$ modes aren't aligned in a straight ridge due to mixed mode as in figure 2(c).

These spectra are fitted using Bayesian analysis, assuming a background model of the spectra that depends on frequencies, splitting, inclination etc. Algorithms like Monte Carlo Markov Chain are used to find the best fitting parameters of the spectra. Some of these parameters can be correlated to each other like inclination and splitting. Hence, estimating one parameter can effect the estimate and errors of other parameters.

3 Convolutional Neural Network (CNN)

Artificial neural networks are inspired by and modelled on biological counterparts. Artificial neurons are functions that take inputs from prior layers, outputting a function of the sum of weighted inputs. These functions may be linear but are generally non-linear, e.g. tanh, sigmoid, reLU etc [16][18]. Neurons have